CHEMISTRY OF MATERIALS

Article

pubs.acs.org/cm

Dual Functionalized Cages in Metal−Organic Frameworks via Stepwise Postsynthetic Modification

Baiyan Li,[†,‡] Dingxuan Ma,[†] Yi Li,[†] Yiming Zhang,[†] Guanghua Li,[†] Zhan Shi,[*,†] Shouhua Feng,[†] Michael J. Zaworotko,[*,‡,§] and Shengqian Ma[*,‡]

[†]State Key Laboratory of Inorganic Synthesis and Preparative Chemistry, College of Chemistry, Jilin University, Changchun 130012, China

[‡]Department of Chemistry, University of South Florida, 4202 East Fowler Avenue, Tampa, Florida 33620, United States

[§]Department of Chemical and Environmental Sciences, University of Limerick, Limerick, Ireland

Supporting Information

ABSTRACT: The introduction of bi- or multifunctionality into different cages of metal−organic frameworks (MOFs) has been of great interest because such MOF materials can demonstrate unique properties for various applications. Herein, we report a general strategy for creating different types of functionalized cages in MOFs by exerting control of the size of cage windows. Selective cage decoration was thereby enabled in such a manner that dual functional MOFs with different types of cages and pores can be created. The resultant different pore function MOF, DPF-MOF, is illustrated as a "proof of concept" in MOF MIL-101-Cr. An intermediate of a cascade reaction was successfully trapped and controlled the desired reaction direction. This DPF-MOF represents a new type of platform that, by trapping intermediates during the reaction processes, enhances our fundamental understanding of reaction chemistry in porous materials.

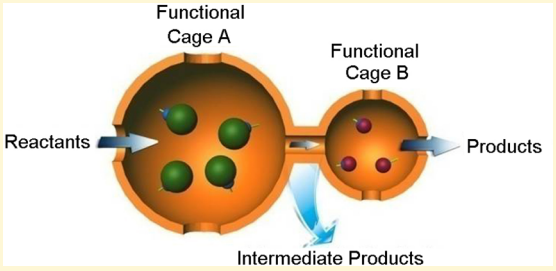

INTRODUCTION

Metal−organic frameworks (MOFs),[1−3] an emerging class of porous materials, have attracted great attention from both academia and industry because of their potential applications in areas as diverse as gas storage,[4,5] separation,[6−8] carbon capture,[9−12] sensing,[13−15] and catalysis.[16−18] Compared with conventional porous materials such as zeolites and mesoporous silica materials,[19,20] MOFs feature greater structural diversity,[21−24] amenability to design,[25−27] adjustable pore size and porosity,[28,29] much larger surface areas,[30−32] a crystalline nature for elucidation of structure−function relationships,[16−18,33,34] and relatively facile immobilization of guest species.[35−38] These features allow MOFs to serve as a new type of platform that can be designed such that they incorporate bi- or multifunctional features into one system for various applications, e.g., cascade catalysis.[39−49] However, MOFs that exhibit two different types of functional pores or cages remain understudied.[50−52] A biporous MOF with different pore function (DPF) (designated herein as DPF-MOFs) is a difficult task if the synthetic approach is exploiting preassembled molecular building blocks (MBBs), despite the large library of organic ligands that can be used to link MBBs. This is because even a small change in the functionality in the linker often leads to the formation of a completely different porous network. Herein, we report the selective functionalization of two different cages based on stepwise postsynthetic modification (PSM).[53−58] This approach is facilitated by the inherent modularity and amenability to PSM of MOFs permitted by porosity. Specifically, grafting different functions into two distinct pore systems has been permitted by window-size control to afford a family of DPF-MOFs.

Our approach to creating DPF-MOFs is based upon exploiting a MOF containing two distinct cages with different window sizes (Scheme 1a) and is accomplished through pore size-controlled stepwise PSM. In the first step, functionality is introduced into both cages via nonselective PSM (Scheme 1b). In the second step, size-controlled selective encapsulation of molecules that can diffuse only into the larger cage creates a cage with one type of function (Scheme 1c). In the third step, the smaller cage is decorated with a different function (Scheme 1d). It is realistic to assert that PSM might be used in an iterative manner to further modify either or both cages, but that is not a focus of this study.

RESULTS AND DISCUSSION

Synthesis and Characterization. To establish a proof of principle for our pore size-controlled stepwise strategy, we selected MIL-101-Cr $\{Cr_3(F)(H_2O)_2O[(CO_2)\text{-}C_6H_4(CO_2)]_3\}$.[59] MIL-101-Cr exhibits **mtn** topology, and as is the case for many MOFs based upon polyhedral cages, it is

Received: May 11, 2016
Revised: June 8, 2016
Published: June 13, 2016

DOI: 10.1021/acs.chemmater.6b01898
Chem. Mater. 2016, 28, 4781−4786

Scheme 1. General Stepwise Strategy for Creating DPF-MOFs[a]

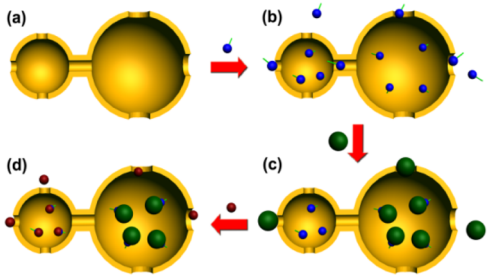

[a](a) Start with a MOF with two types of cages. (b) Use PSM to introduce functionality (blue spheres) into both cages. (c) Size selective PSM (green spheres) involving the large cage only. (d) Use PSM (brown spheres) involving the small cage only.

comprised of more than one type of cage: a 2.9 nm diameter cage that exhibits pentagonal windows with an opening of ~1.2 nm × 1.2 nm and a 3.3 nm diameter cage that possesses both pentagonal windows and larger hexagonal windows with a free aperture of ~1.4 nm × 1.6 nm. The smaller cage and the larger cage are interconnected through the pentagonal windows. The possibility of size selective encapsulation into the larger cage, the presence of unsaturated metal centers (UMCs),[56,57] and organic linkers[60−63] with functional organic groups all contribute to make MIL-101-Cr an ideal candidate for validating whether it is feasible to create DPF-MOFs.

A DPF-MOF with both acidic and basic functionality was prepared by the following process. Ethylenediamine (ED) was first grafted onto the UMCs of MIL-101-Cr to form MIL-101-ED with basic functionality in both cages using procedures detailed in the literature.[56] Elemental analysis revealed that ~1.92 ED per formula unit is present in MIL-101-ED. Phosphotungstic acid ($H_3PW_{12}O_{40}$) (PW) with a 1.35 nm van der Waals diameter was then selectively encapsulated into the larger cages[64] of MIL-101-ED (Scheme 2 and Scheme S1).

Scheme 2. Illustration of the Route for Synthesizing Acid/Base DPF-MOF MIL-101-ED-PW

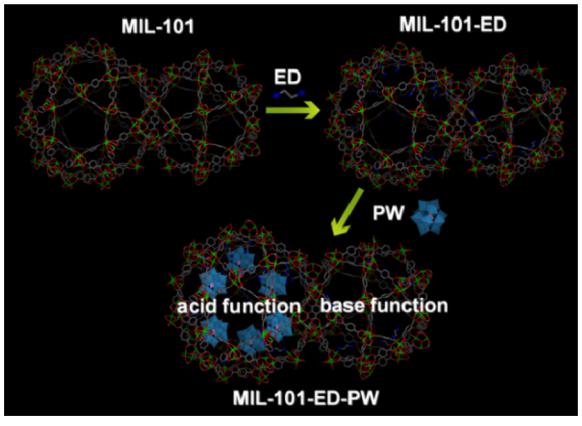

Inductively coupled plasma (ICP) studies indicated ~0.053 Keggin acid anion per Cr(III), which corresponds to 5.6 PWs per large cage (Scheme S1). The encapsulated PW anions are expected to exhibit acid function because of the pseudoliquid phase characteristics of polyacids within pores.[65] A DPF-MOF, MIL-101-ED-PW, was thereby afforded.

Powder X-ray diffraction (PXRD) studies revealed that MIL-101-ED exhibits a PXRD pattern that closely matches that of as-prepared MIL-101-Cr whereas MIL-101-ED-PW is consistent with as-prepared MIL-101-Cr given the expected effect of the PW anions on peak intensities (Figure 1 and Figure S1).[37]

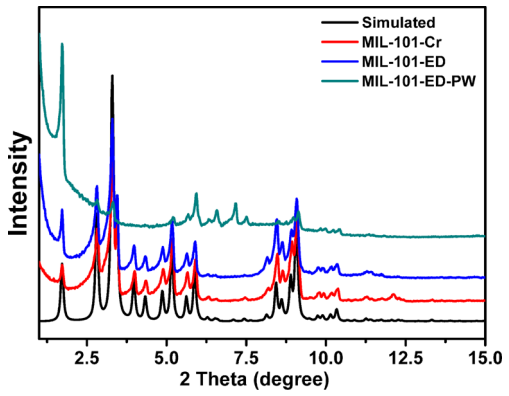

Figure 1. PXRD of MIL-101-Cr (simulated), MIL-101-Cr (as synthesized), MIL-101-ED, and MIL-101-ED-PW.

These results indicate retention of the framework structure after PSM. The FT-IR spectra of dehydrated MIL-101-ED and MIL-101-ED-PW exhibit N−H stretching bands at 3320 cm^{-1}, aliphatic C−H stretching vibrations at 2950 cm^{-1}, and C−N stretching bands at 1054 cm^{-1} (Figure 2),[56] suggesting that

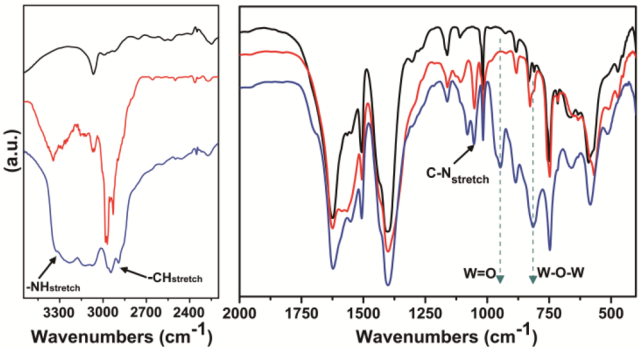

Figure 2. FT-IR spectra of dehydrated samples under vacuum (left) and FT-IR spectra of as-synthesized samples with KBr tablets (right): MIL-101-Cr (black), MIL-101-ED (red), and MIL-101-ED-PW (blue).

EDs were indeed grafted to MIL-101-Cr and retained after the second PSM process. In addition, W−O−W and W═O stretching bands at 815 and 951 cm^{-1}, respectively, for MIL-101-ED-PW correspond to the characteristic bands of PW (Figure 2).[66] The presence of the amino groups and PW anions was also supported by XPS analysis. XPS peaks at 134.7, 36.1, and 38.2 eV from $P^{5+}(2p_{1/2})$, $W^{6+}(4f_{7/2})$, and $W^{6+}(4f_{5/2})$,[67] respectively, further support encapsulation of PW molecules into pores of the MOF (Figure S2). N_2 sorption isotherms (Figure 3) revealed the decrease in BET surface area following stepwise conversion of MIL-101-Cr (BET surface area of 2977 $m^2\ g^{-1}$) to MIL-101-ED (1769 $m^2\ g^{-1}$) to MIL-101-ED-PW (403 $m^2\ g^{-1}$). To verify that the PW anions had indeed diffused into the structure but not on the surface, a thin section containing MIL-101-ED-PW crystals was analyzed by high-resolution transmission electron microscopy with an instrument equipped with an energy dispersive X-ray spectrometer

DOI: 10.1021/acs.chemmater.6b01898
Chem. Mater. 2016, 28, 4781−4786

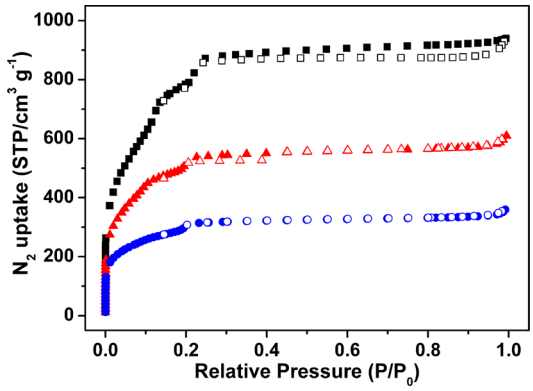

Figure 3. N_2 adsorption−desorption isotherms for MIL-101-Cr (black), MIL-101-ED (red), and MIL-101-ED-PW (blue).

(HRTEM-EDS) (Figure S4). The data revealed a uniform distribution of PW in three random samples. In addition, the content (Table S1) of W/Cr in each layer after XPS reduction treatment is similar, further suggesting the uniform distribution of PW anions throughout the inner pores of MIL-101-ED-PW.

The successful creation of DPF-MOF was also proven by its performance in the cascade reaction. As can be seen from Table S2, MIL-101-ED-PW can catalyze a cascade reaction involving acid-catalyzed deprotection and a subsequent base-catalyzed Henry reaction.[40] The PW in the large cage will catalyze the first step of the reaction, and the ED base sites in the small pore are proposed to catalyze the second step of the reaction. Control experiments with MIL-101-PW or MIL-101-ED further illustrate the advantage of DPF-MOF compared with the monofunctional ones.

Extension of the Pore Size-Controlled Strategy in Creating a DPF-MOF. Our strategy of selective nanospace decoration can also be extended to functional organic molecules to facilitate the creation of a DPF-MOF family with a greater diversity of functionalities. This was accomplished by window size-controlled immobilization of tetrasulfophthalocyanine (Zn) (TSP) (molecular dimensions of ∼1.5 nm × 1.5 nm) into the large cage of MIL-101-Cr,[68] thereby affording MIL-101-ED-TSP following procedures similar to those used earlier (Scheme S2a and Figures S5−S7). MIL-101-ED-TSP was also found to exhibit two functional cages because it can also catalyze the deacetalization−Henry cascade reaction to form **3** (Table S2, entry 4), further highlighting the versatility of our strategy.

Control Experiments Concerning Size-Controlled Selective Decoration. To illustrate the effectiveness of our strategy based on the pore size control, we have conducted a control experiment. An addition of excess PW and TSP during the encapsulation process did not quench the activity of the catalyst as evidenced by our observation that the performances of MIL-101-ED-PW (excess) and MIL-101-ED-TSP (excess) in the deacetalization−Henry cascade reaction are comparable to those of MIL-101-ED-PW and MIL-101-ED-TSP (Table S2, entries 5 and 6, respectively, and Scheme 3a). In contrast, the excess 1,5-naphthalenedisulfonic acid (NDSA), which possesses similar acidic functionality but much smaller molecular dimensions (∼0.9 nm × 1.0 nm), resulted in a loss of activity for MIL-101-ED-NDSA (Table S2, entry 7, and Scheme 3b). We attribute this behavior to the formation of ion pairs at the basic sites. These observations further emphasize that two distinct types of functional cages can be created by the pore

Scheme 3. Stepwise PSM Approach for Constructing DPF Materials with or without Pore Size Control[a]

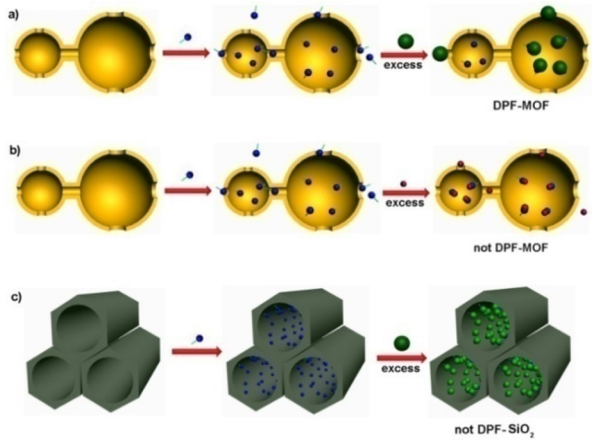

[a](a) Affords DPF-MOFs because of the order and type of reagents used in the process. (b) Monofunctional materials without pore size control because of the small reactant size. (c) Monofunctional materials without pore size control because of the larger windows size for small functional molecules.

size-controlled stepwise strategy presented herein. This contrasts with mesoporous silica materials such as SBA-15[69] that, without pore size control, cannot effectively segregate and differentiate acidic and basic sites under similar conditions (Table S2, entries 8 and 9, respectively, and Scheme 3c).

Further PSM of the Small Cages in MIL-101-NH_2 by the Pore Size-Controlled Strategy. To further illustrate the versatility of our strategy for creating DPF-MOFs with adjusting functions for small cages, we prepared MIL-101-NH_2,[62] a variant of MIL-101-Cr in which amino groups are grafted onto the phenyl ring of the terephthalate linker ligand. PW anions were encapsulated into the large cage of MIL-101-NH_2 using procedures similar to those detailed above. The remaining amino groups in the small cage were then reacted with bromoethylamine to afford MIL-101-$NHCH_2CH_2NH_2$-PW (Scheme S2b and Figures S8−S10). Catalytic studies revealed that two functions were successfully modified. This can be verified because MIL-101-$NHCH_2CH_2NH_2$-PW catalyzes the cascade deacetalization−Henry reaction, whereas MIL-101-NH_2-PW catalyzes only the first step of the cascade reaction (Table S2, entries 10 and 11).

Trapping of a Reaction Intermediate. A model reaction for trapping the intermediate of the cascade reaction was conducted using an amine-Lewis acid system (Figure 4). The amine-catalyzed reaction often generates a mixture of nitroalkene and dinitro products, the latter being the product of further addition of nitroalkane. A Lewis acid catalyst such as Ni(II)-bis[(*R*,*R*)-*N*,*N*′-dibenzylcyclohexane-1,2-diamine]Br_2 (Ni-BDCDBr) can trap the nitroalkene intermediate and direct it toward the formation of a second product, thus preventing the generation of the dinitro product.[70] Ni-BDCDBr (∼1.4 nm × 1.6 nm)[71] was encapsulated into the larger cage of MIL-101-ED as validated by PXRD, IR, N_2 sorption, and XPS (Scheme S2c and Figures S11−S14). Catalytic studies revealed that MIL-101-ED-Ni-BDCDBr can indeed trap the nitroalkene intermediate and form the corresponding Michael addition product. Specifically, MIL-101-ED-Ni-BDCDBr catalyzes reaction of benzaldehyde, nitromethane, and malononitrile to form compound **5** in 91% yield but without the formation of **4**. In

DOI: 10.1021/acs.chemmater.6b01898
Chem. Mater. 2016, 28, 4781−4786

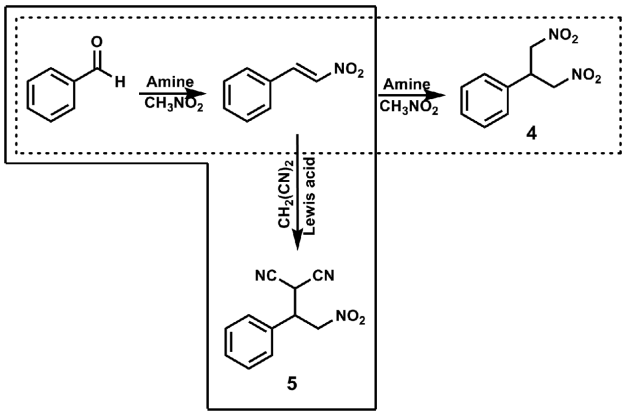

Figure 4. Scheme showing the amine-Lewis acid system for trapping the nitroalkene intermediate [dinitro (---) vs Michael addition product (—)].

contrast, mixtures of ED and Ni-BDCDBr lead to deactivation of Ni-BDCDBr. This can be attributed to the strong chelating effect of ED. The Michael addition product was not detected under such circumstances. Therefore, DPF-MOFs with different functions can be used not only for cascade reactions but also for trapping an intermediate and controlling the reaction route. To the best of our knowledge, this is the first report of reaction intermediate trapping in a functionalized MOF.

Size Selectivity Experiments and Recycling of DPF-MOF. To verify that reactions occur within the DPF-MOF (pore catalysis) instead of on the exterior surface (surface catalysis), size selective catalysis experiments were performed on MIL-101-ED-PW. The Knoevenagel reaction of benzaldehyde and malononitrile in the presence of MIL-101-ED-PW was completed within 3 h, whereas almost no Knoevenagel products were observed if a larger substrate such as diphenylmethanone was used (Table S4 and Figure S15). Additionally, the heterogeneous nature of MIL-101-ED-PW was supported by the observation of no significant loss of activity after three cycles (Table S2, entry 12). Moreover, the fact that the reaction did not proceed after hot filtration is consistent with no leaching of active species and a homogeneous reaction. The content of acid (W = 26.67%) and basic (N = 4.09%) sites after three cycles of catalysis was consistent with the as-synthesized ones with W (28.06%) and N (4.27%) confirmed by elemental analysis and ICP experiments. In addition, the PXRD peak matches that of the as-synthesized samples after reaction well, indicating the intact integrity of the structure (Figure S18).

CONCLUSIONS

In summary, we herein demonstrate pore size-controlled selective decoration of MOF cages through a stepwise PSM process that creates a DPF-MOF comprised of two different types of functional cages. This facile PSM strategy controls the functionalities of the large and small cages of MIL-101-Cr. The stepwise PSM strategy might also be applied to construct "two-in-one" functional MOF materials for other applications in gas storage, separation, sensing, etc. Ongoing work in our laboratories includes the exploration of new functionalities in DPF-MOFs for applications in catalysis and small molecule recognition as well as the development of new strategies for introducing bi- and multifunctionalities into MOFs.

EXPERIMENTAL SECTION

Synthesis of MIL-101-ED-PW. A methanolic solution (10 mL) of phosphotungstic acid (0.15 g, 0.17 mmol) was added to the water solution (30 mL) of MIL-101-ED (0.3 g, 0.45 mmol), and the mixture was stirred at room temperature for 1 h. The product was recovered by filtration, washed with methanol and hot water, and then dried at room temperature. Element analysis: C, 26.47%; H, 2.21%; N, 4.27%. Element analysis after three cycles: C, 27.17%; H, 2.35%; N, 4.09%. ICP: Cr, 12.37%; W, 28.06%. ICP after three cycles: Cr, 11.64%; W, 26.67%.

Synthesis of MIL-101-ED-TSP. The same synthetic procedure that was used for MIL-101-ED-PW was used except that phosphotungstic acid was replaced with tetrasulfophthalocyanine zinc. Element analysis: C, 42.23%; H, 3.26%; N, 6.32%. ICP: Cr, 14.10%; Zn, 1.85%.

Synthesis of MIL-101-ED-Ni-BDCDBr. The same synthetic procedure that was used for MIL-101-ED-PW was used except that PW was replaced with Ni-BDCDBr and CH_2Cl_2 was used as the solvent. Element analysis: C, 46.58%; H, 4.26%; N, 6.79%. ICP: Cr, 14.33%; Ni, 1.95%.

One-Pot Deacetalization–Henry Reaction. A mixture of benzaldehyde dimethyl acetal (1 mmol), nitromethane (5 mL), and catalyst [50 mg, contained free ED (4.2 mg) and PW (18 mg)] was kept at 90 °C under magnetic stirring. The reaction mixture was then stirred under a nitrogen atmosphere for 24 h, and the sample mixture was removed with a filter syringe and evaluated by high-performance liquid chromatography (HPLC) to determine the yield. The strong peak for an equal amount reactant and product was used to calibrate the yield.

One-Pot Deacetalization–Knoevenagel Reaction. A mixture of benzaldehyde dimethyl acetal (1 mmol), malonitrile (2 mmol), and 50 mg of catalyst in toluene (25 mL) was kept at 90 °C under magnetic stirring. The reaction mixture was then stirred under a nitrogen atmosphere for 3 h, and the sample mixture was removed with a filter syringe and evaluated by HPLC to determine the yield. The strong peak for an equal amount reactant and product was used to calibrate the yield.

Experiment with MIL-101-ED-Ni-BDCDBr as a Catalyst for Trapping the Intermediate. A mixture of catalyst (50 mg), benzaldehyde (1 mmol), nitromethane (2.5 mL), malononitrile (1.2 mmol), and toluene (2.5 mL) was kept at 110 °C under magnetic stirring for 24 h. The sample mixture was removed with a filter syringe and evaluated by HPLC to determine the yield. The strong peak for an equal amount reactant and product was used to calibrate the yield.

ASSOCIATED CONTENT

Supporting Information

The Supporting Information is available free of charge on the ACS Publications website at DOI: 10.1021/acs.chemmater.6b01898.

Additional experimental details, characterization data, and simulations (PDF)

AUTHOR INFORMATION

Corresponding Authors

*E-mail: zshi@jlu.edu.cn.
*E-mail: sqma@usf.edu.
*E-mail: xtal@ul.ie.

Notes

The authors declare no competing financial interest.

ACKNOWLEDGMENTS

This work was supported by the National Natural Science Foundation of China (20971054, 90922034, and 21131002), the Specialized Research Fund for the Doctoral Program of Higher Education (20110061110015), the National High

DOI: 10.1021/acs.chemmater.6b01898
Chem. Mater. 2016, 28, 4781–4786

Technology Research and Develop Program (863 program) of China (2013AA031702), the China Postdoctoral Science Foundation (2011M500599), and Special Funding of the China Postdoctoral Science Foundation (2012T50268). Financial support from the University of South Florida and the National Science Foundation (DMR-1352065) is also acknowledged (S.M.). M.J.Z. acknowledges the Science Foundation of Ireland (13/RP/B2549). We thank Prof. Qisheng Huo (Jilin University) for his kind support and advice.

REFERENCES

(1) Kitagawa, S.; Kitaura, R.; Noro, S.-I. Functional Porous Coordination Polymers. *Angew. Chem., Int. Ed.* **2004**, *43*, 2334−2375.
(2) Férey, G. Hybrid Porous Solids: Past, Present, Future. *Chem. Soc. Rev.* **2008**, *37*, 191−214.
(3) Zhou, H.-C.; Long, J. R.; Yaghi, O. M. Introduction to Metal−Organic Frameworks. *Chem. Rev.* **2012**, *112*, 673−674.
(4) Wu, H.; Gong, Q.; Olson, D. H.; Li, J. Commensurate Adsorption of Hydrocarbons and Alcohols in Microporous Metal Organic Frameworks. *Chem. Rev.* **2012**, *112*, 836−868.
(5) Xiang, S.; Zhou, W.; Zhang, Z.; Green, M. A.; Liu, Y.; Chen, B. Open Metal Sites within Isostructural Metal−Organic Frameworks for Differential Recognition of Acetylene and Extraordinarily High Acetylene Storage Capacity at Room Temperature. *Angew. Chem., Int. Ed.* **2010**, *49*, 4615−4618.
(6) Zhao, X.; Bu, X.; Wu, T.; Zheng, S.-T.; Wang, L.; Feng, P. Selective Anion Exchange with Nanogated Isoreticular Positive Metal-Organic Frameworks. *Nat. Commun.* **2013**, *4*, 2344.
(7) Li, J.-R.; Sculley, J.; Zhou, H.-C. Metal−Organic Frameworks for Separations. *Chem. Rev.* **2012**, *112*, 869−932.
(8) Xiang, S. C.; Zhang, Z.; Zhao, C. G.; Hong, K.; Zhao, X.; Ding, D. R.; Xie, M. H.; Wu, C. D.; Das, M. C.; Gill, R.; Thomas, K. M.; Chen, B. Rationally Tuned Micropores within Enantiopure Metal−Organic Frameworks for Highly Selective Separation of Acetylene and Ethylene. *Nat. Commun.* **2011**, *2*, 204.
(9) Sumida, K.; Rogow, D. L.; Mason, J. A.; McDonald, T. M.; Bloch, E. D.; Herm, Z. R.; Bae, T.-H.; Long, J. R. Carbon Dioxide Capture in Metal−Organic Frameworks. *Chem. Rev.* **2012**, *112*, 724−781.
(10) Nugent, P.; Belmabkh-out, Y.; Burd, S. D.; Cairns, A. J.; Luebke, R.; Forrest, K.; Pham, T.; Ma, S.; Space, B.; Wojtas, L.; Eddaoudi, M.; Zaworotko, M. J. Porous Materials with Optimal Adsorption Thermodynamics and Kinetics for CO_2 Separation. *Nature* **2013**, *495*, 80−84.
(11) Xiang, S.; He, Y.; Zhang, Z.; Wu, H.; Zhou, W.; Krishna, R.; Chen, B. Microporous Metal-Organic Framework with Potential for Carbon Dioxide Capture at Ambient Conditions. *Nat. Commun.* **2012**, *3*, 954.
(12) Biswal, B. P.; Panda, T.; Banerjee, R. Solution Mediated Phase Transformation (RHO to SOD) in Porous Co-Imidazolate based Zeolitic Framework With High Water Stability. *Chem. Commun.* **2012**, *48*, 11868−11870.
(13) Takashima, Y.; Martínez, V. M.; Furukawa, S.; Kondo, M.; Shimomura, S.; Uehara, H.; Nakahama, M.; Sugimoto, K.; Kitagawa, S. Unveiling Thermal Transitions of Polymers in Subnanometre Pores. *Nat. Commun.* **2010**, *1*, 83.
(14) Cui, Y.; Yue, Y.; Qian, G.; Chen, B. Luminescent Functional Metal−Organic Frameworks. *Chem. Rev.* **2012**, *112*, 1126−1162.
(15) Lin, R.-B.; Li, F.; Liu, S.-Y.; Qi, X.-L.; Zhang, J.-P.; Chen, X.-M. A Noble-Metal-Free Porous Coordination Framework with Exceptional Sensing Efficiency for Oxygen. *Angew. Chem., Int. Ed.* **2013**, *52*, 13429−13433.
(16) Yoon, M.; Srirambalaji, R.; Kim, K. Homochiral Metal−Organic Frameworks for Asymmetric Heterogeneous Catalysis. *Chem. Rev.* **2012**, *112*, 1196−1231.
(17) Zou, R.-Q.; Sakurai, H.; Xu, Q. Preparation, Adsorption Properties, and Catalytic Activity of 3D Porous Metal−Organic Frameworks Composed of Cubic Building Blocks and Alkali-Metal Ions. *Angew. Chem., Int. Ed.* **2006**, *45*, 2542−2546.
(18) Zhu, C.; Yuan, G.; Chen, X.; Yang, Z.; Cui, Y. Chiral Nanoporous Metal−Metallosalen Frameworks for Hydrolytic Kinetic Resolution of Epoxides. *J. Am. Chem. Soc.* **2012**, *134*, 8058−8061.
(19) Davis, M. E. Ordered Porous Materials for Emerging Applications. *Nature* **2002**, *417*, 813−821.
(20) Shiju, N. R.; Alberts, A. H.; Khalid, S.; Brown, D. R.; Rothenberg, G. Mesoporous Silica with Site-Isolated Amine and Phosphotungstic Acid Groups: A Solid Catalyst with Tunable Antagonistic Functions for One-Pot Tandem Reactions. *Angew. Chem., Int. Ed.* **2011**, *50*, 9615−9619.
(21) Tian, D.; Chen, Q.; Li, Y.; Zhang, Y.-H.; Chang, Z.; Bu, X.-H. A Mixed Molecular Building Block Strategy for the Design of Nested Polyhedron Metal−Organic Frameworks. *Angew. Chem., Int. Ed.* **2014**, *53*, 837−841.
(22) Moulton, B.; Zaworotko, M. J. From Molecules to Crystal Engineering: Supramolecular Isomerism and Polymorphism in Network Solids. *Chem. Rev.* **2001**, *101*, 1629−1658.
(23) O'Keeffe, M.; Yaghi, O. M. Deconstructing the Crystal Structures of Metal−Organic Frameworks and Related Materials into Their Underlying Nets. *Chem. Rev.* **2012**, *112*, 675−702.
(24) Mallick, A.; Garai, B.; Diaz, D. D.; Banerjee, R. Hydrolytic Conversion of a Metal−Organic Polyhedron into a Metal−Organic Framework. *Angew. Chem., Int. Ed.* **2013**, *52*, 13755−13759.
(25) An, J.; Farha, O. K.; Hupp, J. T.; Pohl, E.; Yeh, J. I.; Rosi, N. L. Metal-Adeninate Vertices for the Construction of an Exceptionally Porous Metal-Organic Framework. *Nat. Commun.* **2012**, *3*, 604.
(26) Yaghi, O. M.; O'Keeffe, M.; Ockwig, N. W.; Chae, H. K.; Eddaoudi, M.; Kim, J. Reticular Synthesis and the Design of New Materials. *Nature* **2003**, *423*, 705−714.
(27) Zhao, D.; Timmons, D. J.; Yuan, D. Q.; Zhou, H.-C. Tuning the Topology and Functionality of Metal−Organic Frameworks by Ligand Design. *Acc. Chem. Res.* **2011**, *44*, 123−133.
(28) Lin, X.; Telepeni, I.; Blake, A. J.; Dailly, A.; Brown, C. M.; Simmons, J. M.; Zoppi, M.; Walker, G. S.; Thomas, K. M.; Mays, T. J.; Hubberstey, P.; Champness, N. R.; Schröder, M. High Capacity Hydrogen Adsorption in Cu(II) Tetracarboxylate Framework Materials: The Role of Pore Size, Ligand Functionalization, and Exposed Metal Sites. *J. Am. Chem. Soc.* **2009**, *131*, 2159−2171.
(29) Liu, L.; Konstas, K.; Hill, M. R.; Telfer, S. G. Programmed Pore Architectures in Modular Quaternary Metal−Organic Frameworks. *J. Am. Chem. Soc.* **2013**, *135*, 17731−17734.
(30) Feng, D.; Gu, Z.-Y.; Li, J.-R.; Jiang, H.-L.; Wei, Z.; Zhou, H.-C. Zirconium-Metalloporphyrin PCN-222: Mesoporous Metal−Organic Frameworks with Ultrahigh Stability as Biomimetic Catalysts. *Angew. Chem., Int. Ed.* **2012**, *51*, 10307−10310.
(31) Farha, O. K.; Özgür Yazaydın, A. Ö.; Eryazici, I.; Malliakas, C. D.; Hauser, B. G.; Kanatzidis, M. G.; Nguyen, S. T.; Snurr, R. Q.; Hupp, J. T. De Novo Synthesis of a Metal-Organic Framework Material Featuring Ultrahigh Surface Area and Gas Storage Capacities. *Nat. Chem.* **2010**, *2*, 944−948.
(32) Deng, H.; Grunder, S.; Cordova, K. E.; Valente, C.; Furukawa, H.; Hmadeh, M.; Gándara, F.; Whalley, A. C.; Liu, Z.; Asahina, S.; Kazumori, H.; O'Keeffe, M.; Terasaki, O.; Stoddart, J. F.; Yaghi, O. M. Large-Pore Apertures in a Series of Metal-Organic Frameworks. *Science* **2012**, *336*, 1018−1023.
(33) Cho, S. H.; Ma, B. Q.; Nguyen, S. T.; Hupp, J. T.; Albrecht-Schmitt, T. E. A Metal−Organic Framework Material that Functions as an Enantioselective Catalyst for Olefin Epoxidation. *Chem. Commun.* **2006**, 2563−2565.
(34) Hasegawa, S.; Horike, S.; Matsuda, R.; Furukawa, S.; Mochizuki, K.; Kinoshita, Y.; Kitagawa, S. Three-Dimensional Porous Coordination Polymer Functionalized with Amide Groups Based on Tridentate Ligand: Selective Sorption and Catalysis. *J. Am. Chem. Soc.* **2007**, *129*, 2607−2614.
(35) Aijaz, A.; Karkamkar, A.; Choi, Y. J.; Tsumori, N.; Rönnebro, E.; Autrey, T.; Shioyama, H.; Xu, Q. Immobilizing Highly Catalytically Active Pt Nanoparticles inside the Pores of Metal−Organic Framework: A Double Solvents Approach. *J. Am. Chem. Soc.* **2012**, *134*, 13926−13929.

DOI: 10.1021/acs.chemmater.6b01898
Chem. Mater. 2016, 28, 4781−4786

(36) Lykourinou, V.; Chen, Y.; Wang, X.-S.; Meng, L.; Hoang, T.; Ming, L.-J.; Musselman, R. L.; Ma, S. Immobilization of MP-11 into a Mesoporous Metal−Organic Framework, MP-11@mesoMOF: A New Platform for Enzymatic Catalysis. *J. Am. Chem. Soc.* **2011**, *133*, 10382−10385.
(37) Sun, C.-Y.; Liu, S.-X.; Liang, D.-D.; Shao, K.-Z.; Ren, Y.-H.; Su, Z.-M. Highly Stable Crystalline Catalysts Based on a Microporous Metal−Organic Framework and Polyoxometalates. *J. Am. Chem. Soc.* **2009**, *131*, 1883−1888.
(38) Li, B.; Zhang, Y.; Ma, D.; Ma, T.; Shi, Z.; Ma, S. Metal-Cation-Directed de Novo Assembly of a Functionalized Guest Molecule in the Nanospace of a Metal−Organic Framework. *J. Am. Chem. Soc.* **2014**, *136*, 1202−1205.
(39) Vermoortele, F.; Ameloot, R.; Vimont, A.; Serre, C.; De Vos, D. E. An Amino-Modified Zr-Terephthalate Metal−Organic Framework as an Acid−Base Catalyst for Cross-Aldol Condensation. *Chem. Commun.* **2011**, *47*, 1521−1523.
(40) Li, B.; Zhang, Y.; Ma, D.; Li, L.; Li, G.; Li, G.; Shi, Z.; Feng, S. A Strategy toward Constructing a Bifunctionalized MOF Catalyst: Post-Synthetic Modification of MOFs on Organic Ligands and Coordinatively Unsaturated Metal Sites. *Chem. Commun.* **2012**, *48*, 6151−6153.
(41) Srirambalaji, R.; Hong, S.; Natarajan, R.; Yoon, M.; Hota, R.; Kim, Y.; Ho Ko, Y.; Kim, K. Tandem Catalysis with a Bifunctional Site-Isolated Lewis Acid-Brønsted Base Metal−Organic Framework, NH_2-MIL-101(Al). *Chem. Commun.* **2012**, *48*, 11650−11652.
(42) Deng, H.; Doonan, C. J.; Furukawa, H.; Ferreira, R. B.; Towne, J.; Knobler, C. B.; Wang, B.; Yaghi, O. M. Multiple Functional Groups of Varying Ratios in Metal−Organic Frameworks. *Science* **2010**, *327*, 846−850.
(43) Li, P.; Yu, Y.; Liu, H.; Cao, C.-Y.; Song, W.-G. A Core−Shell−Satellite Structured Fe_3O_4@MS−NH_2@Pd Nanocomposite: A Magnetically Recyclable Multifunctional Catalyst for One-Pot Multistep Cascade Reaction Sequences. *Nanoscale* **2014**, *6*, 442−448.
(44) Lee, Y.-R.; Chung, Y.-M.; Ahn, W.-S. A New Site-Isolated Acid−Base Bifunctional Metal−Organic Framework for One-Pot Tandem Reaction. *RSC Adv.* **2014**, *4*, 23064−23067.
(45) Khajavi, H.; Stil, H. A.; Kuipers, H. P. C. E.; Gascon, J.; Kapteijn, F. Shape and Transition State Selective Hydrogenations Using Egg-Shell Pt-MIL-101(Cr) Catalyst. *ACS Catal.* **2013**, *3*, 2617−2626.
(46) Chen, Y.-Z.; Zhou, Y.-X.; Wang, H.; Lu, J.; Uchida, T.; Xu, Q.; Yu, S.-H.; Jiang, H.-L. Multifunctional PdAg@MIL-101 for One-Pot Cascade Reactions: Combination of Host−Guest Cooperation and Bimetallic Synergy in Catalysis. *ACS Catal.* **2015**, *5*, 2062−2069.
(47) Dhakshinamoorthy, A.; Garcia, H. Cascade Reactions Catalyzed by Metal Organic Frameworks. *ChemSusChem* **2014**, *7*, 2392−2410.
(48) Zhao, M.; Deng, K.; He, L.; Liu, Y.; Li, G.; Zhao, H.; Tang, Z. Core−Shell Palladium Nanoparticle@Metal−Organic Frameworks as Multifunctional Catalysts for Cascade Reactions. *J. Am. Chem. Soc.* **2014**, *136*, 1738−1741.
(49) Rasero-Almansa, A. M.; Corma, A.; Iglesias, M.; Sánchez, F. One-Pot Multifunctional Catalysis with NNN-Pincer Zr-MOF: Zr Base Catalyzed Condensation with Rh-Catalyzed Hydrogenation. *ChemCatChem* **2013**, *5*, 3092−3100.
(50) Ohmori, O.; Kawano, M.; Fujita, M. A Two-in-One Crystal: Uptake of Two Different Guests into Two Distinct Channels of a Biporous Coordination Network. *Angew. Chem., Int. Ed.* **2005**, *44*, 1962−1964.
(51) Kawano, M.; Kawamichi, T.; Haneda, T.; Kojima, T.; Fujita, M. The Modular Synthesis of Functional Porous Coordination Networks. *J. Am. Chem. Soc.* **2007**, *129*, 15418−15419.
(52) Mohideen, M. I.; Xiao, B.; Wheatley, P. S.; McKinlay, A. C.; Li, Y.; Slawin, A. M.; Aldous, D. W.; Cessford, N. F.; Düren, T.; Zhao, X.; Gill, R.; Thomas, K. M.; Griffin, J. M.; Ashbrook, S. E.; Morris, R. E. Protecting Group and Switchable Pore-Discriminating Adsorption Properties of a Hydrophilic−Hydrophobic Metal−Organic Framework. *Nat. Chem.* **2011**, *3*, 304−310.
(53) Cohen, S. M. Postsynthetic Methods for the Functionalization of Metal−Organic Frameworks. *Chem. Rev.* **2012**, *112*, 970−1000.
(54) Wang, Z.; Cohen, S. M. Postsynthetic Modification of Metal−Organic Frameworks. *Chem. Soc. Rev.* **2009**, *38*, 1315−1329.
(55) Lun, D. J.; Waterhouse, G. I. N.; Telfer, S. G. A General Thermolabile Protecting Group Strategy for Organocatalytic Metal−Organic Frameworks. *J. Am. Chem. Soc.* **2011**, *133*, 5806−5809.
(56) Hwang, Y.; Hong, D.-Y.; Chang, J.-S.; Jhung, S. H.; Seo, S. Y.-K.; Kim, J.; Vimont, A.; Daturi, M.; Serre, C.; Férey, G. Amine Grafting on Coordinatively Unsaturated Metal Centers of MOFs: Consequences for Catalysis and Metal Encapsulation. *Angew. Chem., Int. Ed.* **2008**, *47*, 4144−4148.
(57) Deshpande, R. K.; Minnaar, J. L.; Telfer, S. G. Thermolabile Groups in Metal−Organic Frameworks: Suppression of Network Interpenetration, Post-Synthetic Cavity Expansion, and Protection of Reactive Functional Groups. *Angew. Chem., Int. Ed.* **2010**, *49*, 4598−4602.
(58) Banerjee, M.; Das, S.; Yoon, M.; Choi, H. J.; Hyun, M. H.; Park, S. M.; Seo, G.; Kim, K. Postsynthetic Modification Switches an Achiral Framework to Catalytically Active Homochiral Metal−Organic Porous Materials. *J. Am. Chem. Soc.* **2009**, *131*, 7524−7525.
(59) Férey, G.; Mellot-Draznieks, C.; Serre, C.; Millange, F.; Dutour, J.; Surblé, S.; Margiolaki, I. A Chromium Terephthalate-Based Solid with Unusually Large Pore Volumes and Surface Area. *Science* **2005**, *309*, 2040−2042.
(60) Henschel, A.; Gedrich, K.; Kraehnert, R.; Kaskel, S. Catalytic Properties of MIL-101. *Chem. Commun.* **2008**, 4192−4194.
(61) Hong, D.-Y.; Hwang, Y. K.; Serre, C.; Férey, G.; Chang, J.-S. Porous Chromium Terephthalate MIL-101 with Coordinatively Unsaturated Sites: Surface Functionalization, Encapsulation, Sorption and Catalysis. *Adv. Funct. Mater.* **2009**, *19*, 1537−1552.
(62) Bernt, S.; Guillerm, V.; Serre, C.; Stock, N. Direct Covalent Post-Synthetic Chemical Modification of Cr-MIL-101 Using Nitrating Acid. *Chem. Commun.* **2011**, *47*, 2838−2840.
(63) Goesten, M. G.; Juan-Alcañiz, J.; Ramos-Fernandez, E. V.; Sai Sankar Gupta, K. B.; Stavitski, E.; van Bekkum, H.; Gascon, J.; Kapteijn, F. Sulfation of Metal−Organic Frameworks: Opportunities for Acid Catalysis and Proton Conductivity. *J. Catal.* **2011**, *281*, 177−187.
(64) Juan-Alcañiz, J.; Ramos-Fernandez, E. V.; Lafont, U.; Gascon, J.; Kapteijn, F. Building MOF Bottles Around Phosphotungstic Acid Ships: One-Pot Synthesis of Bi-functional Polyoxometalate-MIL-101 Catalysts. *J. Catal.* **2010**, *269*, 229−241.
(65) Okuhara, T.; Kasai, A.; Hayakakawa, N.; Yoneda, Y.; Misono, M. Catalysis by Heteropoly Compounds. VI. The Role of the Bulk Acid Sites in Catalytic Reactions over $Na_xH_{3-x}PW_{12}O_{40}$. *J. Catal.* **1983**, *83*, 121−130.
(66) Pazé, C.; Bordiga, S.; Zecchina, A. H_2O Interaction with Solid $H_3PW_{12}O_{40}$: An IR Study. *Langmuir* **2000**, *16*, 8139−8144.
(67) Jalil, P. A.; Faiz, M.; Tabet, N.; Hamdan, N. M.; Hussain, Z. A Study of the Stability of Tungstophosphoric Acid, $H_3PW_{12}O_{40}$, Using Synchrotron XPS, XANES, Hexane Cracking, XRD, and IR Spectroscopy. *J. Catal.* **2003**, *217*, 292−297.
(68) Zalomaeva, O. V.; Kovalenko, K. A.; Chesalov, Y. A.; Mel'gunov, M. S.; Zaikovskii, V. I.; Kaichev, V. V.; Sorokin, A. B.; Kholdeeva, O. A.; Fedin, V. P. Iron Tetrasulfophthalocyanine Immobilized on Metal Organic Framework MIL-101: Synthesis, Characterization and Catalytic Properties. *Dalton Trans.* **2011**, *40*, 1441−1444.
(69) Zhao, D.; Feng, J.; Huo, Q.; Melosh, N.; Fredrickson, G. H.; Chmelka, B. F.; Stucky, G. D. Triblock Copolymer Syntheses of Mesoporous Silica with Periodic 50 to 300 Angstrom Pores. *Science* **1998**, *279*, 548−552.
(70) Poe, S. L.; Kobašlija, M.; McQuade, D. T. Microcapsule Enabled Multicatalyst System. *J. Am. Chem. Soc.* **2006**, *128*, 15586−15587.
(71) Evans, D. A.; Seidel, D. Ni(II)−Bis[(R,R)-N,N′-dibenzylcyclohexane-1,2-diamine]Br_2 Catalyzed Enantioselective Michael Additions of 1,3-Dicarbonyl Compounds to Conjugated Nitroalkenes. *J. Am. Chem. Soc.* **2005**, *127*, 9958−9959.

DOI: 10.1021/acs.chemmater.6b01898
Chem. Mater. 2016, 28, 4781−4786